# Nanostructured Photovoltaic Cell of the Type Titanium Dioxide, Cadmium Sulfide Thin Coating, and Copper Thiocyanate Showing High Quantum Efficiency

Gerardo Larramona,* Christophe Choné, Alain Jacob, Daisuke Sakakura, Bruno Delatouche, Daniel Péré, Xavier Cieren, Masashi Nagino,† and Rocío Bayón‡

*IMRA Europe S.A.S., 220 rue Albert Caquot, F-06904 Sophia Antipolis, France*

*Received December 21, 2005. Revised Manuscript Received January 27, 2006*

Nanostructured photovoltaic devices were fabricated using a porous n-type $TiO_2$ film, a thin layer of CdS acting as the absorber, and a transparent p-type CuSCN filling the pores. The cell showed an internal quantum efficiency of ∼100% and significant cell efficiency of 1.3% at 1 sun, as well as high photovoltage (0.85 V) and a filling factor of 0.65. Though the cell concept was already proposed by others, this cell clearly shows a significant performance and it demonstrates the potentiality of such cells made with very thin absorber layers (<10−20 nm) and largely structured porous films (roughness factor >100). Description of component characterization and explanation of identified issues are presented.

## Introduction

Present photovoltaic systems for roof-top house application are mainly based on crystalline Si technologies, but they are still very expensive. Among alternative low cost technologies, the dye-sensitized solar cell (DSC)[1,2] makes use of new concepts such as nanostructured cell configuration and dye molecule absorbers and has reached conversion efficiencies at lab scale of 5−11% depending on the type of electrolyte. However, DSC still faces problems of stability at high temperatures under full sun irradiation (due to nature of dye and electrolyte) and limitation in cell efficiency.

A new solid-state photovoltaic device called an extremely thin absorber (eta) solar cell was proposed by Könenkamp's team[3,4,5] based on some features of the DSC (nanostructured configuration, separation of light absorption from charge transport) and some of classical photovoltaic devices (solid-state, inorganic materials). It consists of a three-component three-dimensional porous heterojunction of the type "n−a−p" ("a" meaning absorber), in which a thin layer of an inorganic absorber is deposited over the internal surface of a porous film made of a transparent n-type semiconductor, the rest of the pore volume being filled with a transparent p-type semiconductor. Photons are only absorbed by the absorber layer, and the generated electron/hole pairs are injected into the two separate transparent phases, n-type and p-type, respectively. As a consequence of such separation, the chances of charge recombination are highly reduced. On the other hand, if the absorber layer is thin enough (lower than the diffusion length of carriers within the absorber), the absorber material would have much lower restrictions concerning the number of defects.

Theoretically this concept could overcome the limitations of efficiency and stability of DSC keeping the advantage of low cost, but very few trials have been published. Authors of the same team[5] reported a cell made with n-type porous $TiO_2$ films, $CuInS_2$ absorber coating (made by electrodeposition), and CuSCN as transparent the p-type semiconductor filling the pores. However, the conversion efficiency, photocurrent, and spectral response (quantum efficiency) of such cells were very small, even if the dark-current feature of the cells was acceptable. At a similar moment, Tennakone's team[6] reported a nanostructured cell of the type $TiO_2$/Se/CuSCN, though they did not claim to be of the eta type; in fact, from their cell scheme and comments it seemed that the Se film was electrodeposited mainly as a layer on the top of the $TiO_2$ layer opposite to the glass side (rather than inside the $TiO_2$ film) and that the CuSCN layer was deposited just above those layers, without a significant penetration into the $TiO_2$. They reported an efficiency of 0.13%, with a narrow quantum efficiency spectrum (at 600−700 nm, with a window of nearly no response at 400−550 nm), and bad shaped current−voltage curves both under irradiation (very low filling factor, ∼0.05) and under dark. Other later publications[7,8] claimed better results with other examples of extremely thin absorber (eta) solar cells, but the reported

* To whom correspondence should be addressed. E-mail: larramona@imra-europe.com.

† Present address: Aisin Chemical Co., Ltd., Nishikamo, Aichi 470-0492, Japan.

‡ Present address: CIEMAT, av Complutense 22, E-28040 Madrid, Spain.

(1) Grätzel, M. *Chem. Lett.* **2005**, *34*, 8.
(2) O'Regan, B. C.; Grätzel, M. *Nature* **1991**, *414*, 338.
(3) Siebentritt, S.; Ernst, K.; Fischer, C.-H.; Könenkamp, R.; Lux-Steiner, M. C. *Proceedings of the 14th European Photovoltaic Solar Energy Conference & Exhibition*, Barcelona, H. S. Stephens & Ass., Bedford, 1997; p 1823.
(4) Rost, C.; Ernst, K.; Siebentritt, S.; Könenkamp, R.; Lux-Steiner, M. C. *Proceedings of the 2nd World Conference & Exhibition Photovoltaic Solar Energy Conversion*, Vienna, Joint Research Center European Commission, Ispra, 1998; p 212.
(5) Kaiser, I.; Ernst, K.; Fischer, C.-H.; Könenkamp, R.; Rost, C.; Sieber, I.; Lux-Steiner, M. Ch. *Sol. Energy Mater. Sol. Cells* **2001**, *67*, 89.
(6) Tennakone, K.; Kumara, G. R. R. A.; Kottegoda, I. R. M.; Perera, V. P. S.; Aponsu, G. M. L. P. *J. Phys. D: Appl. Phys.* **1998**, *31*, 2326.
(7) Belaidi, A.; Bayón, R.; Dloczik, L.; Ernst, K.; Lux-Steiner, M. Ch.; Könenkamp, R. *Thin Solid Films* **2003**, *431−432*, 488.
(8) Ernst, K.; Belaidi, A.; Könenkamp, R. *Semicond. Sci. Technol.* **2003**, *18*, 475.

10.1021/cm052819n CCC: $33.50 
Published on Web 02/24/2006

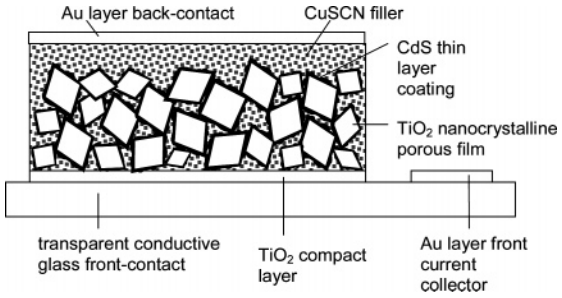


**Figure 1.** Schematic of the nanostructured solar cell.

photovoltaic devices were in fact based on a different concept, consisting on a two-component cell with the n-type porous film (such $TiO_2$) and an absorber filling the pores, but without the transparent p-type component such as CuSCN. Recently, a conversion efficiency of ~2% was reported by Lévy-Clément's team[9] for a photovoltaic device close to the eta concept, made with a porous ZnO film (composed of vertically aligned prismatic columns of ~100−200 nm width and 1−2 $\mu$m height), a coating of CdSe absorber (of ~40 nm thickness), and CuSCN filling the pores. This structure, however, has a small internal surface (roughness factor <10), which limits the maximum amount of absorber coating, and it uses an absorber layer which is rather thick, which will enhance the losses by charge recombination inside such a layer if defects are not well-controlled.

Therefore, there seems to be no clear demonstration yet on the potentiality to get high efficiencies with extremely thin absorber photovoltaic devices which use very thin absorber layers (<10−20 nm) and porous n-type semiconductor films of high internal surface (roughness factor > ~100). Here we report results that clearly indicate the possibility of obtaining high efficiencies with such a solid-state photovoltaic concept, by means of a cell configuration made with a highly porous $TiO_2$ film, a thin coating of CdS absorber, and a filler of CuSCN p-type transparent semiconductor. The CdS absorber has a narrow absorption spectrum (yellow color), but it can be considered as a model material to obtain a clear demonstration of the potentiality of such a cell concept. In addition to its narrow spectrum we are aware that CdS (as any Cd containing compound) is a toxic material (see hazards explanation below), and current trends in several countries try to limit (or even ban) its industrial use.

## Experimental Section

A schematic of the whole cell is shown in Figure 1. Porous films were made with anatase $TiO_2$ nanocrystals. Suspensions of such crystals were prepared in-house by a sol−gel method using Ti alcoxide precursors obtained by previously described methods.[10] Our particular sol−gel method was based on aqueous alkaline media, the details being described elswhere.[11] The colloids had a broad particle size dispersion ranging from ~20 to ~200 nm, the average size being tuned by synthesis parameters such as pH and autoclave temperature and time, or with sequential centrifugation after synthesis. Different types of colloids were thoroughly investigated. One was finally chosen as the standard, having an average particle size of ~40−50 nm (the equivalent BET active surface being ~ 30−40 $m^2/g$). Data reported here were obtained with such a standard colloid, unless otherwise stated. Porous films were prepared by doctor blade[11] followed by sintering at 450−480 °C. The film thickness was tuned from 2 to 10 $\mu$m, the typical value being 3 $\mu$m. Films were translucent whitish, significantly scattering the light, which contributed to enhance light absorption by the absorber coating. The film roughness factor (internal area over projected one) was ~50−100 per $\mu$m of film thickness (e.g., 150−300 for a 3 $\mu$m thick film).

Commercial F-doped $SnO_2$ transparent conductive glasses from Asahi Glass were used as substrates for $TiO_2$ film deposition. Prior to nanocrystalline film deposition, a compact layer of $TiO_2$ of ~50−60 nm thickness was deposited by spray pyrolysis of Ti alcoxide precursor solutions;[12] an in-house setup was made to allow automatic and reproducible coatings over areas as large as 10 × 10 cm. This barrier layer was needed to avoid holes from CuSCN being collected in the conductive glass front contact. The different parameters controlling the automatic setup as well as the optimum layer thickness were optimized for such barrier layer fabrication.

Deposition of CdS coating was based on solution deposition, which is a low cost technique known for the fabrication of thin films on flat substrates. Two types of solution deposition techniques were investigated: sequential chemical bath deposition (S-CBD), also known as SILAR (successive ionic layer adsorption and reaction), and chemical bath deposition (CBD). Preliminary trials with several flat substrates as well as several nanocrystalline porous films ($TiO_2$ and other metal oxides) showed that the recipes could not be transferred from one substrate to another. In the case of the S-CBD method, several $Cd^{2+}$ salts and $S^{2-}$ containing compounds and different solution concentrations and immersion times were investigated. Finally, a standard recipe was chosen as follows: The sample was successively immersed in four different beakers for about 30 s each; one contained a 0.05 M $Cd(NO_3)_2$ aqueous solution, another contained 0.05 M $Na_2S$, and the other two contained distilled water to rinse the samples from the excess of each precursor solution. Such an immersion cycle was repeated several times, typically between 5 and 20 cycles. After several cycles the film became a strong yellow to orange. In the case of CBD, single solutions containing a $Cd^{2+}$ salt, thiourea as the $S^{2-}$ precursor, and different complexants were investigated. Samples made with CBD showed lower light absorption and cell performance than those samples obtained by S-CBD. Then, data reported herein will concern samples obtained with the S-CBD method. Concerning CdS hazards we should mention that Cd metal, Cd oxide, CdS, and other Cd salts and compounds are considered toxic by different regulations; the main hazard for humans is that they can be carcinogens mainly by long inhalation exposure (suspended dusts in air, not because of volatility), the main target organs being the kidneys and lungs, and in particular, burning of wastes would produce fumes containing Cd oxide. However, the main reason to limit Cd use seems to be its effect on the environment because Cd salts are very toxic to aquatic media. There are, though, defenders of its usage who argue that hazards and disposals can be well-controlled and recyclability is easy and economic.

The $TiO_2$ films were usually pretreated (before CdS coating) with Al tributoxide[13] so as to leave a very thin $Al_2O_3$ coating, which could act as a buffer layer to reduce back recombination.

(9) Lévy-Clément, C.; Tena-Zaera, R.; Ryan, M. A.; Katty, A.; Hodes, G. *Adv. Mater.* **2005**, *17*, 1512.
(10) Barbé, Ch. J.; Arendse, F.; Comte, P.; Jirousek, M.; Lenzmann, F.; Shklover, V.; Grätzel, M. *J. Am. Ceram. Soc.* **1997**, *80*, 3157.
(11) Choné, Ch.; Larramona, G.; Sakakura, D. European Patent EP1271580 A1, 2003.
(12) Kavan, L.; Grätzel, M. *Electrochim. Acta* **1995**, *40*, 643.
(13) Palomares, E.; Clifford, J. N.; Haque, S. A.; Lutz, T.; Durrant, J. R *Chem. Commun.* **2002**, 1464.

The CuSCN filling was done by impregnation and evaporation following the method described to fabricate solid DSCs of the type $TiO_2$/dye/CuSCN.[14,15] Instead of a manual impregnation, a machine similar to that described elsewhere[15] was built and used to carry out an automatic and better-controlled CuSCN filling. Several designs of dispenser tubing as well as different deposition conditions were studied. In our final standard method, a solution of ~0.07 M CuSCN in propyl sulfide was spread on the top of the $TiO_2$/CdS film while keeping it hot at 80 °C and by moving the dispenser tubing forward and backward several times. The time/amount of CuSCN deposition was adjusted not only to fill the pores but also to leave an overlayer of CuSCN on the top (thickness between 10 nm and 1 $\mu$m), which was necessary to avoid any shortcuts between the $TiO_2$/CdS layer and the back-contact. Prior to CuSCN deposition, the films were impregnated with a 0.5 M LiSCN aqueous solution, wiped off, and dried at 80 °C.

The cell fabrication was finished by depositing a gold layer of ~40 nm thickness by means of an Edwards 306 Evaporator. This gold layer was deposited in two regions: one over the CuSCN layer, so as to be used as the back-contact, and the other in the $TiO_2$-free zone on the conductive glass substrate, so as to be used as the front-contact current collector. The cell was placed in a sample holder for its characterization with the current−voltage and the spectral response setups. Contact to the gold layers was made by means of pressed nickel foams. The sample holder contained a mask placed on the top of the cell, which was used to have an exact and fixed illuminated active surface of 0.54 $cm^2$ (5 × 9 mm), the actual cell surface being slightly superior.

The following machines and setups were used for the characterization of components and cells. Absorption spectra were recorded with a Perkin-Elmer Lambda-20 spectrophotometer with an integrated sphere accessory. The current−voltage cell characterization was measured with an in-house setup designed and calibrated so as to closely follow the international photovoltaic standards (norm IEC 904-3). Measurements were carried out typically at an irradiance of ~100% sun (= 1000 $W/m^2$) and ~10% sun as well as in the dark. Quantum efficiencies were measured by an in-house setup ranging from 400 to 1100 nm wavelength. Its software allowed the calculation of the mismatch factor of the lamp with respect to the standard sun spectrum AM1.5G, which was input in the current−voltage setup to obtain accurate measurements. Scanning electron microscopy (SEM) images were acquired with a Hitachi S-4700 field-emission scanning electron microscope, to which an EDX (energy-dispersive X-ray microanalysis) Noran System SIX was coupled. Transmission electron microscopy (TEM) images were acquired with a JEOL 2010 FEG-200kV microscope, to which an EDX Oxford Isis was coupled. Ionization potentials were measured with an ultraviolet photoelectron spectroscopy (UPS) Riken Keiki AC-2. X-ray diffraction (XRD) plots were measured with a Philips PW 1710 machine with Cu Kα radiation.

## Results and Discussion

**Spectral Response.** The absorption spectra of the $TiO_2$/CdS films were measured by UV−visible spectroscopy using an integrating sphere accessory. Absorption spectra of samples with ~10 cycles of CdS deposition showed large light absorption and an absorption onset at ~560 nm (2.2 eV), which is at slightly longer wavelengths than the literature band gap of bulk CdS (2.4−2.5 eV).[16,17] The optical band gap could not be exactly inferred from these spectra due to the scattering nature of the films. For thick $TiO_2$ films (>6 $\mu$m) and a large enough amount of CdS (>10 cycles CdS deposition), the absorption spectra were squarelike and attained 100% absorption over the ~400−500 nm plateau (~15% absorption was due to the conductive glass substrate). The maximum photocurrent expected from those spectra (assuming 100% photon conversion) was calculated to be ~6.5 $mA/cm^2$ by using the standard solar spectrum AM1.5G.

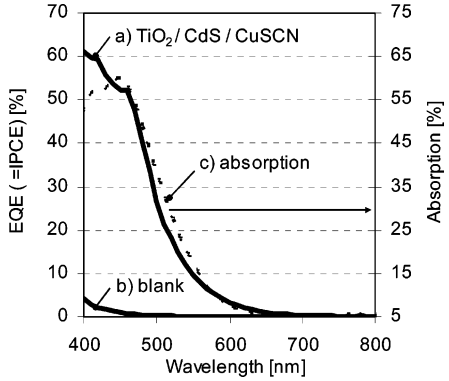


**Figure 2.** EQE (=IPCE) of (a) the $TiO_2$/CdS/CuSCN cell and (b) the $TiO_2$/CuSCN blank cell, compared to (c) the absorption spectrum of the $TiO_2$/CdS film.

The spectral response of one of the best cells is shown in Figure 2 as the external quantum efficiency (EQE) versus the wavelength, also known as IPCE (incident photon-to-current conversion efficiency). The maximum value of the EQE was ~60%, which is a very high value, and the integrated photocurrent was 3.3 $mA/cm^2$. Figure 2 also shows the light absorption spectrum of the same cell before CuSCN deposition (after correction by the absorption spectrum of the conductive glass/$TiO_2$ substrate). Both EQE and the absorption spectrum are nearly coincident, which implies that the cell showed a maximum internal quantum efficiency (IQE) of ~100% (IQE can be roughly calculated by normalizing EQE with respect to the absorption spectrum corresponding to the absorber; IQE is also known as APCE, absorbed photon to current conversion efficiency). This result indicates that such a new nanostructured device has a good potentiality.

Non-negligible quantum efficiencies were reported with photoelectrochemical cells made with metal oxide films ($TiO_2$ etc.) having adsorbed CdS quantum dots (QDs), either made ex situ and incorporated into the metal oxide film[18] or with QDs made in situ with solution deposition techniques[19] as in here. Those photoelectrochemical cells were completed with aqueous liquid electrolytes (hence, they were not stable) and using a three-electrode electrochemical cell. The reported EQE (= IPCE) can be considered as a tool to evaluate the electron injection of the QDs into the metal oxide film (also known as the semiconductor sensitization phenomenon), but this tool is not enough to confirm the functioning of solid-state devices such as the one of the present paper. On the

(14) Kumara, G. R. A.; Konno, A.; Senadeera, G. K.; Jayaweera, P. V.; De Silva, D. B.; Tennakone, K. *Sol. Energy Mater. Sol. Cells* **2001**, *69*, 195.
(15) O'Regan, B. C.; Lenzmann, F. *J. Phys. Chem. B* **2004**, *108*, 4342.
(16) Xu, Y.; Schoonen, M. A. *Am. Mineral.* **2000**, *85*, 543.
(17) Memming, R. *Philips Tech. Rev.* **1978/1979**, *38*, 160.
(18) Peter, L. M.; Riley, D. J.; Tull, E. J.; Wijayantha, K. G. U. *Chem. Commun.* **2002**, *1030*.
(19) Vogel, R.; Hoyer, P.; Weller, H. *J. Phys. Chem.* **1994**, *98*, 3183.

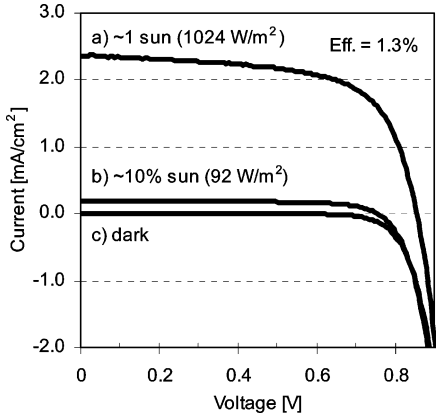


**Figure 3.** Current/voltage curves of the $TiO_2$/CdS/CuSCN cell at (a) ~1 sun, (b) ~10% sun, and (c) in the dark.

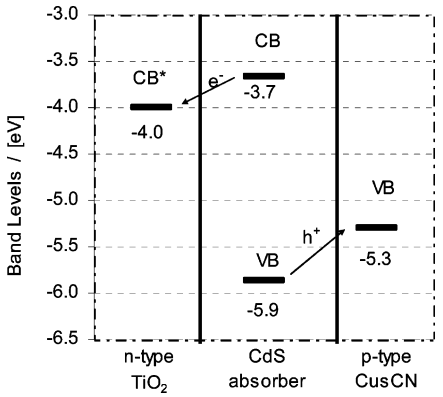


**Figure 4.** Measured energy band levels of components of the $TiO_2$/CdS/CuSCN cell; CB* of $TiO_2$ was taken from the literature; CB of the CdS coating was calculated by adding the absorption onset of 2.2 eV to the VB value; and VB values were measured as ionization potentials.

other hand, the QDs cell targets a film with isolated dots, which is different from the concept of the eta solar cell.

**Cell Efficiency.** The conversion efficiency of the cells was measured by the current−voltage ($I-V$) curves under illumination. Figure 3 shows the $I-V$ curves and conversion efficiencies of one of the best cells. The cell efficiency was 1.3% at ~1 sun (photocurrent $J_{sc} = 2.3$ mA/cm$^2$, open-circuit voltage $V_{oc} = 0.86$ V, filling factor ff = 0.65). Both $I-V$ curves at ~100% and ~10% sun as well as the dark-current curve have the shape expected for classical photovoltaic devices. Besides the significant $J_{sc}$ (taking into account that CdS is a narrow absorber), the other factors, $V_{oc}$ and ff, were quite high. These results together with the previous quantum efficiency result represent, then, a clear demonstration of the good potentiality of such a solar cell concept.

**Energy Band Diagram.** Figure 4 shows the energy band diagram corresponding to this cell of three components. Similarly to what has been explained for other nanostructured solar cells such as dye-sensitized cells,[20] it is very likely that no appreciable band bending takes place in any phase due to the small particle size of every component (typically <50 nm). The valence band (VB) values of CdS and CuSCN were directly assigned from the values of the ionization potential obtained with the UPS spectrometer: −5.9 eV for the CdS coating (measuring a $TiO_2$/CdS sample) and −5.3 eV for

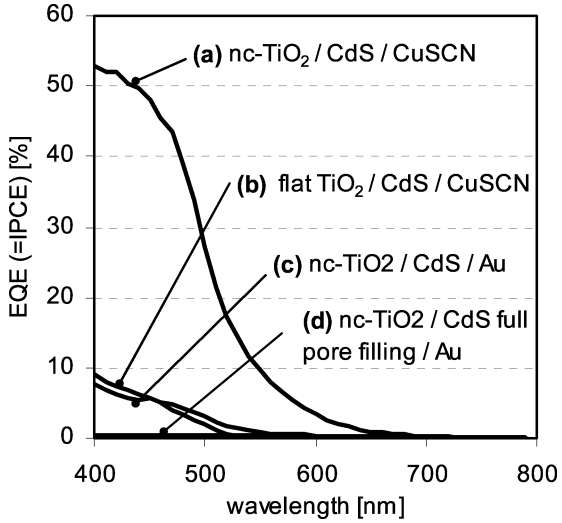


**Figure 5.** EQE (=IPCE) of different cell configurations: (a) nanocrystalline $TiO_2$/CdS/CuSCN; (b) flat compact layer $TiO_2$/CdS/CuSCN; (c) nanocrystalline $TiO_2$/CdS/Au (without CuSCN, CdS is the thin coating); (d) sample in part c but with nearly full CdS pore filling.

CuSCN (measuring a $TiO_2$/CuSCN sample). The first value is similar to that obtained for bulk CdS powder with the same machine, while the second value is 0.3 eV higher than the VB value of bulk CuSCN powder. The conduction band (CB) of CdS was calculated by adding the absorption onset (2.2 eV) to the VB value. We propose to use the measured absorption onset instead of the literature band gap (2.4−2.5 eV) because it would be the less favorable case and it will take into account more real absorbed photons. The VB of the $TiO_2$ film could not be measured since it was outside the energy range of the apparatus; a literature data point of −4.0 eV[21] was taken for the CB of $TiO_2$, although it is known that such a value can change[16,17,21] depending on factors such as the amount of adsorbed ions such $OH^-$ (which can be changed with treatments with solutions of different pH). According to the mechanism proposed for other types of nanostructured cells, the CB of the absorber should be located "above" (closer to the vacuum level) the CB level of the n-type semiconductor ($TiO_2$), and the VB of the absorber should be located "below" the VB of the p-type semiconductor (CuSCN). In such a way, electrons and holes can be transferred from the absorber to the respective transparent semiconductors. The energy band diagram obtained here fulfills such conditions, which is in agreement with the good quantum efficiency obtained with this cell.

**Comparison with Other Cell Configurations.** An item of concern in this type of cell is the question whether carriers are traveling through the transparent semiconductor phases or one carrier is traveling through the absorber layer (one transparent phase being inactive). To obtain some answer, different cell configurations were quickly investigated and their quantum efficiencies were compared (see Figure 5). A cell with a flat layer configuration was made with a compact $TiO_2$ layer without the nanocrystalline (nc-$TiO_2$) layer and with flat CdS and CuSCN layers. It showed a maximum EQE < 10% and a cell efficiency < 0.1% (Figure 5b), that is,

(20) Cahen, D.; Hodes, H.; Grätzel, M.; Guillemoles, J. F.; Riess, I. *J. Phys. Chem. B* **2000**, *104*, 2053.

(21) Zaban, A.; Micic, O. I.; Gregg, B. A.; Nozik, A. J. *Langmuir* **1998**, *14*, 3153.

much less than the nanostructured cell (Figure 5a). This low efficiency may be due to recombination losses inside the CdS phase because electrons and holes travel in the same phase through a long pathway (CdS film thickness was ~200 nm), compared to the short pathway in the nanostructured cell (CdS coating was ~5 nm, see below). Another cell configuration was a nanostructured cell similar to the standard cell but without the p-type CuSCN and keeping a Au contact on the top. This cell showed a maximum EQE < 10% and a cell efficiency < 0.1% (Figure 5c), that is, much less than the standard nanostructured cell. This means that the CdS/Au contact was probably a Schottky contact to allow hole injection from n-CdS to Au, which would justify the significant EQE (10%). However, the decrease of EQE would be explained because the hole transport should take place in the CdS phase in the absence of the CuSCN phase. Finally, another cell consisted in a cell similar to the previous one (nc-$TiO_2$/CdS/Au) but with CdS filling nearly the whole pore volume. EQE and the cell efficiency were negligible (Figure 5d). In this case, charge recombination inside the CdS phase may have prevailed, because the CdS phase is much thicker (compared to cell type c), as we argued for the flat cell (type b). The fact that the cell is also worse than the flat layer could be due to the much larger path towards the back contact (3 $\mu$m in this cell instead of 200 nm in the flat layer cell). All these results seem to support the hypothesis that charge transport in the present nanostructured cell takes place through the two different n-$TiO_2$ and p-CuSCN phases.

**CdS Coating Nature.** SEM images of $TiO_2$ films before and after CdS deposition showed the presence of the CdS coating as sort of flattened particles were evenly distributed all over the $TiO_2$ crystals. Figure 6 shows an example of $TiO_2$ nanocrystals before and after 15 cycles of CdS deposition. The coating was homogeneous along the $TiO_2$ thickness for films up to ~8 $\mu$m thick, as checked with SEM images taken at different points of the film cross section and also with EDX profiles. For films of >10 $\mu$m, the CdS coating was less dense in the bottom of the film (close to the conductive glass substrate).

TEM images coupled with EDX analysis gave additional information about the coating. Figure 7 shows a TEM image of $TiO_2$/CdS with a medium number of CdS cycles (<10 cycles). First, the presence of small CdS particles or dots of ~5 nm size was confirmed. EDX spectra taken with the beam focused in such dots demonstrated a composition made of Cd and S. Second, the $TiO_2$ crystals appeared to be completely covered by a very thin film of CdS (<1 nm) in addition of the dispersed CdS particles; this was confirmed by EDX by focusing the beam tangentially to the surface of $TiO_2$ crystals in regions without any apparent CdS particle. As the number of CdS cycles increased (15−20 cycles), the number of CdS flattened particles and the average dot size increased just slightly. Therefore, it can be concluded that the coating consisted of an overall coverage of CdS over the $TiO_2$ crystal surface, though the thickness was not uniform but made of a thin layer plus dispersed thicker dots. This picture, then, corresponds more to the idea of the eta solar cell and differs from the idea of the QDs solar cell.

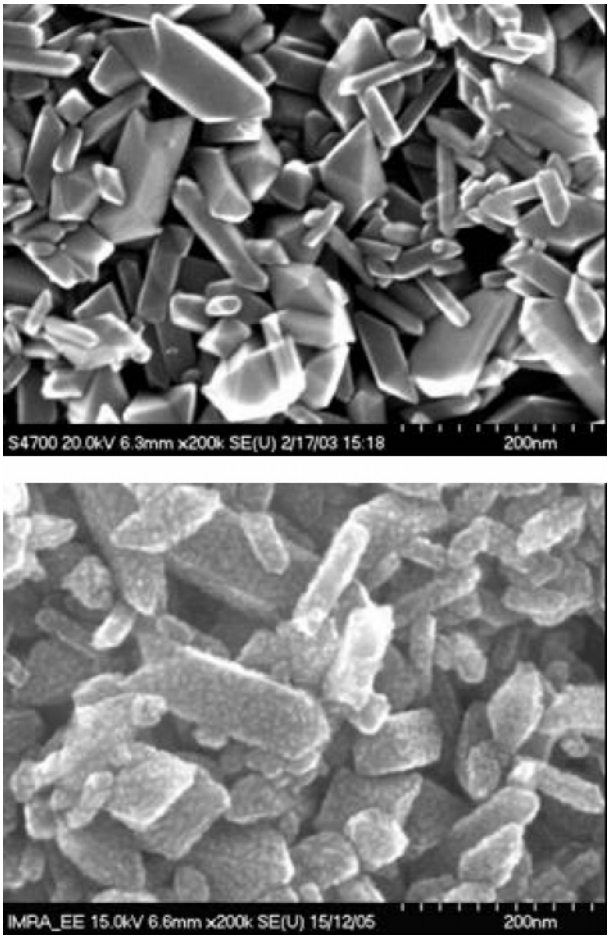


**Figure 6.** SEM images of uncoated nanocrystalline $TiO_2$ film and CdS-coated $TiO_2$ film (15 cycles of CdS coating by S-CBD).

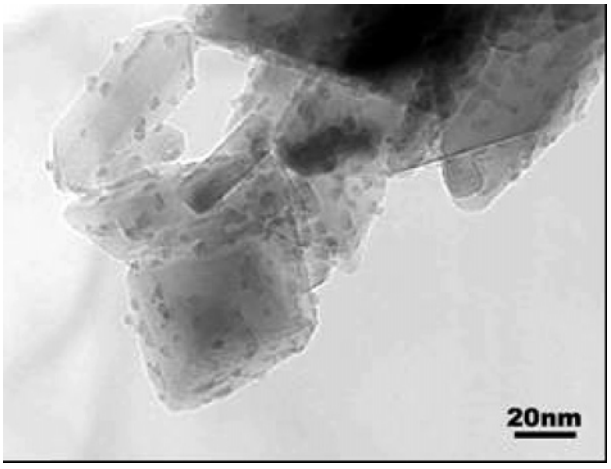


**Figure 7.** TEM image of $TiO_2$/CdS sample (<10 cycles of CdS coating).

Concerning crystallinity, atomic planes could be distinguished in the CdS particles by increasing the magnification of TEM acquisition. However, we should point out that the TEM image was evolving with time, meaning that the beam could be altering the structure of CdS during acquisition. Therefore, the degree of CdS crystallinity inferred from the TEM measurements was somewhat uncertain. Crystallinity was further studied by doing XRD measurements carried out on $TiO_2$ and $TiO_2$/CdS samples with long acquisition times. Three new broad peaks could be observed after CdS deposition (Figure 8), indicating the presence of the cubic

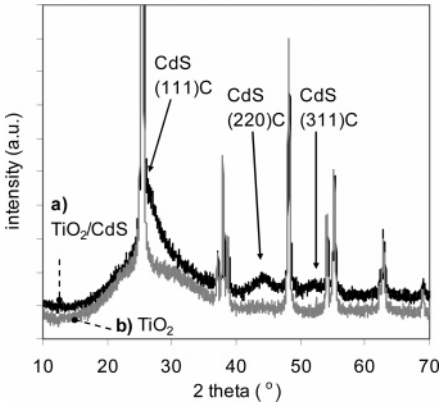


**Figure 8.** XRD of (a) the nanocrystalline $TiO_2$/CdS film and (b) the $TiO_2$ film (both on glass substrates).

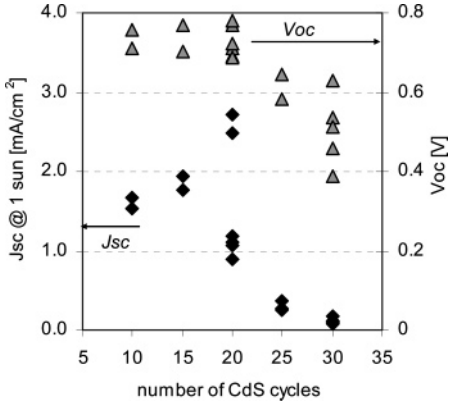


**Figure 9.** Photocurrent ($J_{sc}$) and open-circuit voltage ($V_{oc}$) extracted from $I-V$ curves at 1 sun for the $TiO_2$/CdS/CuSCN cell where the amount of CdS was changed with the number of S-CBD cycles.

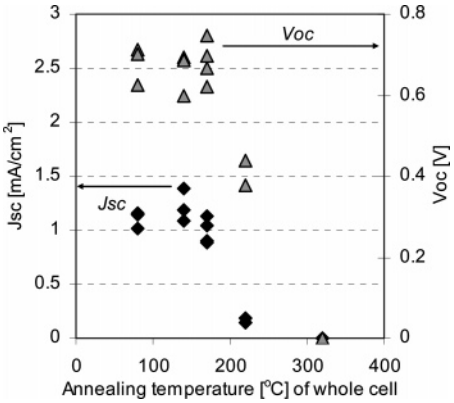


**Figure 10.** Photocurrent ($J_{sc}$) and open-circuit voltage ($V_{oc}$) extracted from $I-V$ curves at 1 sun for $TiO_2$/CdS/CuSCN cells where the whole cell was annealed in a $N_2$ atmosphere at different temperatures.

CdS phase ($a = 5.8304$ Å, JCPDS file 01-089-0440) in $TiO_2$/CdS samples. The rest of the peaks correspond to those of $TiO_2$ anatase (tetragonal phase: $a = 3.7852$ Å and $c = 9.5139$ Å, JCPDS file 00-021-1272). The substrate was soda glass instead of conductive glass so as to avoid extra peaks coming from the F-doped $SnO_2$. We are still not sure about the nature of the very thin coating mentioned above or about the presence of other crystalline or amorphous CdS phases. Further research would be needed to conclude about the impact of the crystallinity of the coating on the cell performance.

**CdS Coating Amount.** The amount of CdS coating was evaluated by EDX analysis coupled with the SEM apparatus. For 15 cycles of CdS coating the atomic ratio Cd/Ti was ~10%. This is equivalent to a volume ratio (CdS over $TiO_2$) of ~15% (molecular weight, MW, of CdS = 144.5 g/mol, MW of $TiO_2$ = 79.9 g/mol, density of $TiO_2$ anatase = 3.84 g/cm$^3$, density of cubic CdS = 4.5 g/cm$^3$). By doing a rough calculation, the equivalent thickness of a CdS coating assuming that it was uniformly distributed with a constant thickness all over the $TiO_2$ crystal surface was estimated to be of the nanometer order. From another point of view, the CdS amount in a typical $TiO_2$ film of 3 $\mu$m thickness is also equivalent to a dense compact layer of 200−300 nm.

Concerning the stoichiometry, the Cd/S atomic ratio obtained by EDX was ~1, but we should point out that the EDX value cannot be considered very accurate, especially if we consider the low amount of absorber compared to that of $TiO_2$. The EDX software delivers deviation values for the calculation of the atomic percentage from the spectra; for example, for the atomic ratio Cd/Ti of 10%, the error given by the program was about ±1% (for a single spectrum). In addition we made EDX measurements on several samples; for each sample, in several zones at 3−4 mm of distance; and for each zone, at different points at 2−3 $\mu$m of distance. The average standard deviation obtained from such different points was Cd/Ti 10% ±1.5%, that is, about 15% relative error. Besides the issue of the precision, there is also some concern about the accuracy, because we checked the Cd/S ratio of pure commercial CdS powders and they showed a variation up to ~10% relative depending on the choice of the acceleration voltage parameter used in the measurement.

One way to increase the amount of absorber was by increasing the number of CdS deposition cycles. Figure 9 shows two factors concerning cell performance as a function of the CdS cycles: the photocurrent at short-circuit ($J_{sc}$) and the open-circuit photovoltage ($V_{oc}$) at 1 sun, extracted from the $I-V$ curves. Although there was some important data scatter (see below), it can be concluded that $J_{sc}$ reached a maximum around 15−20 cycles of CdS deposition. The $V_{oc}$ (which is related to $J_{sc}$ to a certain extent) was high and constant for up to 20 cycles and then decreased. The behavior of $J_{sc}$ can be explained because of the balance of two effects: As the amount of CdS increases, the light absorption increases and so does $J_{sc}$. However, as the thickness of CdS increases, the amount of CuSCN would decrease and also some pores may become unaccessible because they are occluded by CdS particles; in such a case, hole collection and transport in the CuSCN phase would be less effective, making $J_{sc}$ decrease.

**Annealing Effect.** Annealing was investigated as a way to change the nature of the coating (since it can change the CdS dot size or its crystallinity) or a way to improve the interface contact $TiO_2$/CdS and/or CdS/CuSCN. Annealing of either $TiO_2$/CdS films or the whole cells was carried out in a glovebox under a $N_2$ atmosphere to avoid any possible degradation coming from $O_2$ or humidity. Figure 10 shows the performance as $J_{sc}$ and $V_{oc}$ at 1 sun (extracted from the $I-V$ curves). The reference cell (nonannealed) is represented as the "80 °C" annealing temperature because the cells were heated at this temperature during the CuSCN deposition. When annealing the $TiO_2$/CdS film prior to CuSCN deposi-

tion (not shown in Figure 10), the cell efficiency slightly decreased by increasing annealing temperature up to ~220 °C (small decrease in both $J_{sc}$ and $V_{oc}$), and it decreased significantly at higher annealing temperatures. When annealing the whole cell (Figure 10), the cell efficiency was constant up to 170 °C, and it decreased dramatically at higher annealing temperatures. In conclusion, no increase of cell efficiency could be obtained by an annealing step. However, these data show that cells were quite stable at high temperatures, which is not the case of other nanostructured cells using absorbers or hole conductors that are organic or organometallic.

**$TiO_2$ Film Thickness.** Another way to increase the amount of CdS coating was to play with the thickness of the $TiO_2$ film. Several $TiO_2$ film thicknesses from 2 and 10 $\mu$m were studied. Light absorption attained a maximum with the thicker films (>6 $\mu$m keeping constant 15 cycles of CdS). However, cell efficiency did not increase significantly by increasing film thickness. Champion efficiencies were obtained with $TiO_2$ films ranging from 2 to 5 $\mu$m. One reason could be the limitation by the diffusion length of holes along the longer pathways of the CuSCN phase. Another reason could be the increase of electron-hole back-recombination in the regions of thin CdS coating due to the increase of the interface pathway along the film.

**Reproducibility.** We have to point out that though the reported champion data has been 1.3% efficiency at 1 sun, the data scatter was significant. We analyzed data scatter by compiling $I-V$ data obtained in many experiments carried out throughout about 1 year using cells made with the same fabrication conditions, such as a $TiO_2$ film thickness of ~3 $\mu$m and CdS coating of 15 cycles. Values showing abnormally low $V_{oc}$ (certainly due to short-circuiting in cell fabrication) were removed from the analysis. The min−max range (average standard deviation shown in parentheses) corresponding to the four factors of cell performance at 1 sun were the following: $J_{sc}$ = 1−2.5 mA/cm$^2$ (average standard deviation 1.6 ± 0.4), $V_{oc}$ = 0.6−0.8 V (average 0.75 ± 0.05), ff = 0.3−0.6 (average 0.5 ± 0.1), and efficiency = 0.3−1.2% (average 0.6 ± 0.2). This data scatter may look high in relative proportion; however, considering absolute values, scatters of ±0.5% points in efficiency and of ± 1mA/cm$^2$ in $J_{sc}$ are quite common in other technologies (such as a dye-sensitized cell, for which this laboratory has much experience). Reasons of such scatter could not be identified yet, but it could be related to the surface state of the $TiO_2$ film or to changes in the interface contacts aroused from the steps of CdS deposition or CuSCN filling.

**CuSCN Filling.** SEM images of the cell cross section showed pores largely filled with CuSCN, though it was not possible to distinguish clearly any structure. Quantitative evaluation of CuSCN filling percentage was tried by measuring the Cu/Ti atomic ratio with EDX. The Cu/Ti profile was constant over the $TiO_2$ film for thickness up to ~6 $\mu$m. The EDX measurement in the top ~2 $\mu$m of the $TiO_2$ film was higher than in the rest of the film because of the overestimation in that region due to the contribution of the CuSCN overlayer (0.01−1 $\mu$m thick) next to it (the beam spatial resolution was a cube of about 1 $\mu$m$^3$). Therefore, to have more accurate values of the CuSCN amount, EDX measurements were restricted to cross section regions located at least ~1−2 $\mu$m below the top of the $TiO_2$ film.

Homogeneity over the 2.5 × 2.5 cm substrates (note that one substrate was used to fabricate two cells) was initially checked with $TiO_2$/CuSCN films without CdS. Cu/Ti ratios were constant in the direction of the dispenser movement but had a parabolic distribution in the perpendicular direction (Cu/Ti ~ 50−60% in the edges and ~ 15−20% in the middle of the substrate). This was probably caused by the design of the dispenser tube (a single hole in the middle); other designs, though, did not produce better fillings. The average value for the CuSCN filling was taken as the one in the middle of the cell active surface, which corresponded to a Cu/Ti atomic ratio of ~30%. This atomic ratio roughly corresponds to an average of ~50−60% pore volume filling obtained by means of a rough calculation (using a MW of $TiO_2$ = 79.9 g/mol, MW of CuSCN = 121.26 g/mol, density of $TiO_2$ = 3.84 g/cm$^3$, density of CuSCN = 2.85 g/cm$^3$, and 40−50% porosity for the $TiO_2$ films before CuSCN filling). This pore filling percentage was probably enough to ensure a continuous and sufficiently thick path for an efficient hole transport.

Another important factor having a big impact in cell performance was the salt pretreatment prior to CuSCN filling. We found out that the spectral response was quite low in the absence of LiSCN pretreatment ($J_{sc}$ < 0.2 mA/cm$^2$ compared to 3.3 mA/cm$^2$ with pretreatment). Apart from LiSCN, other salts were investigated for such pretreatment, like some $SCN^-$ salts of cations different from $Li^+$ and some $Li^+$ salts of anions different from $SCN^-$. Among those, only KSCN showed the same behavior as LiSCN. Addition of $Li^+$ salts have been suggested to be beneficial for photovoltaic devices such as dye-sensitized cells with liquid electrolytes,[22] organic hole conductors[23] (with the argument that $Li^+$ has either a role of charge screening or that of shifting the CB of $TiO_2$), or light-emitting diodes.[24] In the present case, the presence of $Li^+$ is not essential because a $K^+$ salt showed a similar effect. Therefore, the effect may arise from the $SCN^-$ anion. Some authors[25] suggested the beneficial effect of adding EMISCN salt for solid dye-sensitized cells where CuI was used as a solid electrolyte, in which such a salt would have the role of decreasing the size of the CuI crystals and, hence, improving the interface contact. In the present study, SEM images of cells with and without pretreatment showed similar structures (at least in what concerns the CuSCN overlayer, where some grain boundaries can still be seen). EDX measurements showed a slight decrease in the CuSCN pore filling for the non-pretreated cell, but it was still high enough. Resistivity measurements made by recording current−voltage curves of $TiO_2$/CuSCN films sandwiched between two conductive substrates showed that non-pretreated cells gave much higher

(22) Liu, Y.; Hagfeldt, A.; Xiao, X.-R.; Lindquist, S.-E. *Sol. Energy Mater. Sol. Cells* **1998**, *55*, 267.
(23) Krüger, J.; Plass, R.; Le Cevey, M. P.; Grätzel, M.; Bach, U. *Appl Phys. Lett.* **2001**, *79*, 2085.
(24) Schmitz, C.; Schmidt, H.-W.; Thelakkat, M. *Chem. Mater.* **2000**, *12*, 3012.
(25) Kumara, G. R. A.; Konno, A.; Shiratsuchi, K.; Tsukahara, J.; Tennakone, K. *Chem. Mater.* **2002**, *14*, 954.

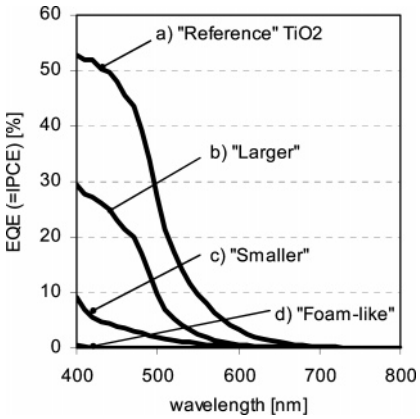


**Figure 11.** EQE (=IPCE) of $TiO_2$/CdS/CuSCN cells with different $TiO_2$ film structure: (a) "Reference" is the standard nanocrystalline film of ~40−50 nm average particle size; (b) "Larger" is ~100 nm average size; (c) "Smaller" is 10−15 nm average size; and (d) "Foamlike" is a porous $TiO_2$ structure resembling a foam with a wide range of pore sizes from 0.5 to 5 $\mu$m.

resistance than pretreated ones. The explanation of the effect of LiSCN (or KSCN) pretreatment may come from such observation in the resistivity: there might be an improvement of interface contact between CuSCN particles favored by the $SCN^-$ salt, or $SCN^-$ might act as a dopant increasing, hence, the conductivity. Further research would be needed to clarify this point.

**Type of $TiO_2$ Nanostructure.** The nature of the $TiO_2$ nanostructure may play a big role in the performance of this type of cell, in particular, the particle and pore sizes. Apart of the extensive research to find our standard colloid, different porous $TiO_2$ films were also investigated. Cells were completed using the same method and similar conditions for depositing CdS and CuSCN. Figure 11 shows the spectral response of a selection of cells made with different $TiO_2$ films, including our standard structure (labeled "Reference" in the figure). One film was a nanocrystalline $TiO_2$ of average particle size of ~100 nm (labeled "Larger") and pore size similar to particle size, obtained by a synthesis similar to that of the Reference but changing slightly the conditions of pH, temperature, and autoclave time so as to allow a further increase of the particle size. Another film was a nanocrystalline $TiO_2$ of average particle size ~10−15 nm, obtained by in-house synthesis using the acetic acid method[10] (labeled "Smaller"). Finally, a porous $TiO_2$ film was made by spray-pyrolysis of a $TiO_2$ colloidal suspension,[26] which resembled a foam structure (labeled "Foamlike") with much larger pores than the other structures, ranging from 0.5 to 5 $\mu$m. The best cell performance was that of the Reference nanocrystalline film. The next best spectral response was that of the film labeled "Larger", though it showed both a spectral response and a cell efficiency of about half those of the reference. This decrease in performance could be due to the lower amount of CdS caused by the lower internal surface of the film. The film labeled "Smaller" had much more internal surface than the reference but five times less spectral response and quite low cell efficiency (<0.1%). EDX measurements in such a sample gave a Cd/Ti atomic ratio of ~10% (similar to that of reference) and a Cu/Ti ratio of ~20% (less than reference, which was ~30%, but still large enough). Therefore, the reason for the bad performance of the film labeled "Smaller" could be the bad conductivity in the CuSCN path due to the small size of the $TiO_2$ film pores or to the bad contact between CdS and CuSCN because of the larger tortuosity of the internal surface of the film. In conclusion, the type of $TiO_2$ structure was confirmed to be a very important factor affecting the cell efficiency: a good tuning of particle and pore sizes is important; there should be enough internal surface to deposit sufficient absorber but also a minimum pore size (and probably a special pore shape) to facilitate CuSCN deposition and create a continuous CuSCN path. This finding could have been a key factor to get such a significant efficiency with this type of cell.

**Buffer Layers.** Teams working on dye-sensitized cells have suggested[13] the concept to cover the $TiO_2$ nanocrystalline film with a thin layer of $Al_2O_3$ (or other insulating materials) to decrease the dark current or the back-recombination. In our standard procedure of cell fabrication we also tried to include an $Al_2O_3$ pretreatment prior to absorber coating. We investigated such a coating with SEM and TEM, but the techniques did not allow any clear thin layer to be distinguished. In addition, Al was detected by EDX (coupled with either SEM or TEM) in only about half of the samples. Taking into account the data scatter of cell performance (see above), we could not conclude whether the $Al_2O_3$ pretreatment was advantageous or not. In any case, cell efficiency > 1% was obtained both with a cell without $Al_2O_3$ pretreatment and with a cell with $Al_2O_3$ pretreatment (and where Al was detected by EDX).

**Stability.** The study of cell stability was complicated by the fact that cell efficiency was low (<1.3%) and data scatter was significant. Therefore, we could not proceed with a full study on cell stability. However, we can say that unsealed cells were stable for several months when left in the lab atmosphere, the loss being about 20%. Unsealed cells which showed ~1% efficiency after fabrication still showed ~0.5% efficiency after 0.5−1 year of being left in the lab. On the other hand, we carried out indirect tests of stability by measuring the absorption spectra of $TiO_2$/CdS/CuSCN films (without the gold layer), sealed with a glass plate substrate and a heat-resistant adhesive. Both light soaking tests (halogen lamp at ~1 sun irradiance) and thermal stress tests at 100 °C showed stable absorption spectra for over 2000 h. These data seem to indicate a promising stability for this kind of cells.

## Conclusions

The results shown above are a clear demonstration of the potentiality of the concept of the nanostructured solar cell based on an eta layer. The reported cell has been made with the model absorber material CdS, for which we cannot probably expect more than 3% cell efficiency because it is a narrow absorber. To progress with this type of cell, it would be necessary first to continue with some fundamental research to clarify the mechanism as well as to investigate

(26) Könenkamp, R.; Ernst, K.; Fischer, Ch.-H.; Lux-Steiner, M. C.; Rost, C. *Phys. Status Solidi A* **2000**, *182*, 151.

additional requirements for the different components and the interfaces. Issues such as the nature of the absorber coating, the type of $TiO_2$ nanostructure, and the properties of the p-type filler are worthwhile to investigate to obtain higher and more reproducible cell efficiencies. A second step would be to demonstrate the potentiality of the same cell concept with an absorber material having a broad spectrum of light absorption, such the materials used in thin-film photovoltaic technologies.

**Acknowledgment.** We thank Dr. Philippe Venneguès (CHREA, CNRS Sophia Antipolis, France) for the discussions on the TEM measurements, Dr. Ramon Tena-Zaera (LCMTR, CNRS Thiais, France) for the discussions on the results of XRD measurements, Dr. Kazuo Higuchi (Toyota Central R&D Labs, Inc., Japan) for the discussions on the ionization potential measurements, and Dr. Brian O'Regan for the clarifications and discussions on the CuSCN filling method.

CM052819N